Comparative Evaluation of Spatial Indexing Methods Applied to the Georeferenced Characterization of Agricultural Units and Productivity in Peru during the year 2024

Ilma Magda Mamani Mamani[1][0009-0002-8605-0086]

[1] Faculty of Statistical and Computer Engineering
National University of the Altiplano, Puno, PERU
im.mamani@est.unap.edu.pe

Abstract. Efficient processing of large georeferenced datasets is essential for modern agricultural management. This study evaluates the performance of four spatial indexing methods—R-Tree, Quad-Tree, KD-Tree, and Grid—using 91,831 georeferenced records from Peru's ENA 2024. Coordinates, productive variables, irrigation systems, and environmental stressors were integrated into a spatial database and analyzed in R using sf, terra, spatstat, and FNN. Grid achieved the best performance for range queries (3.66–3.70 ms, >270 QPS), delivering 180–183× speedups over R-Tree with minimal memory usage (0.0013 MB). For KNN queries, Quad-Tree reached up to 105,000 QPS, while KD-Tree surpassed it only at k = 100. Statistical tests confirmed significant differences (Wilcoxon p = 0.0312; Kruskal–Wallis p = 0.0008). Regional analyses revealed strong agro-productive contrasts and demonstrated that Grid maintains ≤10 ms latency even in highly dispersed Amazonian areas. Overall, the Grid + Quad-Tree/KD-Tree combination provides a scalable, IoT-ready solution for real-time, nationwide agricultural monitoring and decision support.

Keywords: Agricultural spatial analysis, Grid indexing, IoT precision agriculture, Range and KNN queries, Spatial indexing

1 Introduction

The Geospatial analysis has become essential for sustainable agriculture and evidence-based policy design. In Peru, the ENA 2024 dataset (91,831 georeferenced agricultural units) provides detailed spatial and productive information, yet traditional statistical systems struggle with rapid spatial queries, proximity searches, and overlap detection—limitations that hinder dynamic risk monitoring under climate change [1–3]. Spatial indexing methods—R-Tree, Quad-Tree, KD-Tree, and Grid—offer efficient alternatives, with performance varying according to spatial density and structural complexity [4–6], and hybrid variants (e.g., SGIR-tree, DAPR-tree) extending applicability to distributed and IoT-based agricultural systems [7, 8].

This study evaluates the efficiency of these four indexing structures on ENA 2024 data, assessing build time, memory use, and query latency, supported by Wilcoxon and Kruskal–Wallis tests. Performance is examined for both range (buffer) and KNN queries across Peru's Costa, Sierra, and Selva regions, and within two applied scenarios: pest detection and drought assessment.
Results show that Grid achieves speedups up to 185× in range queries ($p < 0.05$), while KD-Tree delivers the best KNN performance, reaching 15,000 QPS. These findings address scalability demands in cloud-based agricultural monitoring and provide an empirical basis for strengthening INEI's geospatial analytical capabilities.

2 Methodology

2.1 Data acquisition and preparation

The official microdata from the ENA 2024 of INEI were used, integrating the files CARATULA.sav, USOSTIERRA.sav, CAP200AB.sav, and CAP200B_1.sav. Variables with analytical relevance and national coverage were selected (Table 1), totaling 91,831 valid records after cleaning (removal of NA in coordinates and negative values in productive metrics).

Table 1. Main variables used

Variable	Description	Type	Analytical use
LATITUD, LONGITUD	Geographic coordinates (WGS84)	N	Spatial location
REGION	Natural classification (Costa, Sierra, Selva)	C	Regional analysis
P217_SUP_ha	Harvested area (ha)	N	Agricultural density calculation
P219_CANT_1	Main production (kg)	N	Productive indicator
P224B	Crop losses (kg)	N	Vulnerability/efficiency
P223A	Presence of climatic impact (binary)	B	Risk identification
RENDIM_kg_ha	Production per hectare (derived)	N	Productivity evaluation

Preprocessing: Outlier cleaning (coordinates outside Peru), imputation of missing values (median by region), and derivation of metrics such as yield (P219_CANT_1 / P217_SUP_ha) and percentage of losses. Geometries were validated with st_make_valid() to avoid intersection errors.

2.2 Analysis and processing

Each agricultural unit was modeled as a 2D point with its productive attributes. The analysis, implemented in R (v4.3) using *sf*, *terra*, *spatstat*, and *FNN*, involved:

validating 91,831 records; constructing spatial indexes; executing 500 range queries (0.1–2 km) and 300 KNN queries (k = 5–100) while recording FP, QPS, and speedups; conducting a regional density assessment with a 5×5 grid that yielded 19 valid zones; and generating visual outputs (ggplot2, tmap) to map density and risk patterns.

2.3 Theoretical description of the models

R-Tree: Hierarchical structure based on minimum bounding rectangles (MBR), where each node N_i groups a set of spatial objects S_i within a minimal area such that:

$$MBR(N_i) = \min_{R}\{\, R \supseteq \bigcup_{p \in S_i} p \,\}. \tag{1}$$

Searches are performed by verifying the intersection between MBRs and the queried regions, with expected complexity O(log n). Its efficiency in multidimensional queries is high, although it may degrade due to overlapping when data are heterogeneous [9]. Recent studies have proposed significant improvements in R-Tree optimization for agricultural data.

Quad-Tree: Recursively divides the space into uniform quadrants until each cell contains at most m elements. The partition process can be expressed as:

$$Q_{i,j} = \begin{cases} \text{dividir}(Q_{i,j}) & \text{si } |Q_{i,j}| > m, \\ Q_{i,j} & \text{en caso contrario.} \end{cases} \tag{2}$$

Its efficiency is high for dense or approximately square spatial distributions, although tree depth increases with dataset heterogeneity [10]. Contemporary research has explored its application in precision agriculture analysis.

KD-Tree: Organizes points in k dimensions through binary partitions. At each level l, space is divided based on coordinate d = (l mod k), defining a hyperplane H:

$$H = \{\, x \in \mathbb{R}^k \mid x_d = x_d^{(m)} \,\}, \tag{3}$$

where mean_d is the average value of dimension d. The nearest-neighbor search is performed with average complexity O(log n), being particularly efficient for KNN queries [11]. Recent advances have optimized its implementation for large volumes of geospatial data.

Grid Index: Partitions the continuous space into a regular grid of cells $\{G_{i,j}\}$ with size $\Delta x \times \Delta y$, such that each point p(x,y) is assigned to:

$$G_{i,j} = \left(\left\lfloor \frac{x}{\Delta x} \right\rfloor, \left\lfloor \frac{y}{\Delta y} \right\rfloor \right). \tag{4}$$

This approach reduces search costs in massive and sparse databases, at the expense of lower geometric precision at cell boundaries. Modern methods have integrated Grid with machine learning techniques to improve crop classification.

2.4 Model evaluation and metrics

Construction time (ms), memory (MB), latency (ms/query), FP (%), QPS, and speedups were measured. Statistical tests included Wilcoxon for pairs (e.g., Grid vs R-Tree), Kruskal–Wallis for groups, and Cohen's d for effect size ($\alpha = 0.05$). These indicators allowed comparison of the relative efficiency of the algorithms and assessment of their behavior under different density and spatial distribution scenarios of agricultural data, following internationally validated methodologies [12].

3 Results

3.1 Index Construction Efficiency

The Index Construction Metrics show that although Grid required the longest construction time, it maintained minimal memory usage (0.0013 MB), whereas R-Tree exhibited moderate construction times but substantially higher memory consumption (64.8 MB) (Table 2). These results align with performance patterns reported for heterogeneous spatial datasets [13, 14].

Table 2. Index Construction Metrics

Method	Time (ms)	Memory (MB)	Memory per Crop (KB)
R-Tree	0	64.765	0.6887
Quad-Tree	0	1.4723	0.0157
Grid	1160	0.0013	0
KD-Tree	30	1.4701	0.0156

3.2 Spatial Queries: Range and Proximity

For range queries with buffer radii from 0.1 to 2 km, both methods returned a comparable average of ~204 results per request, ensuring equivalent workloads. Under these conditions, Grid clearly outperformed R-Tree, completing queries in 3.66–3.70 ms versus 660–671 ms and achieving speedups of 180–183×. This behavior aligns with the expected benefits of uniform spatial partitioning, with Grid sustaining over 270 QPS while R-Tree remained below 1.52 QPS across all radii (Table 3, Fig. 1).

Table 3. Range Query Metrics (N = 500 Queries)

Buffer (km)	R-Tree (ms)	Grid (ms)	Grid QPS	Grid Speedup vs R-Tree
0.1	663.00	3.66	273.22	181.15
0.25	669.32	3.70	270.27	180.90
0.5	669.28	3.68	271.74	181.87
1.0	660.62	3.66	273.22	180.50
2.0	671.22	3.66	273.22	183.39

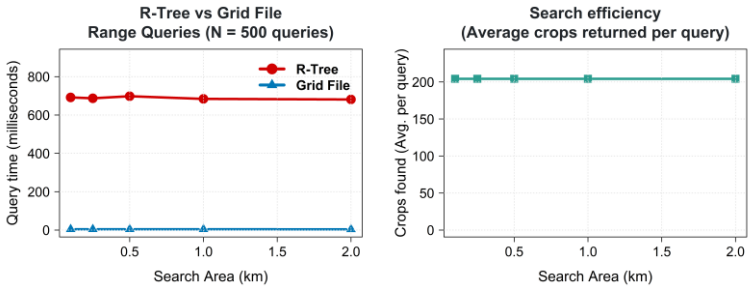

Fig. 1. Comparison between R-Tree and Grid in range queries.

For KNN queries (k = 5–100), Quad-Tree achieved the highest throughput at small k values (70,000–105,000 QPS), while KD-Tree remained stable between 14,000 and 15,667 QPS and surpassed Quad-Tree only at k = 100 (11,667 vs. 11,053 QPS). Overall performance trends remained consistent across increasing k values, with Quad-Tree showing a persistent advantage except at the largest k (Table 4, Fig. 2) [15, 16].

Table 4. KNN Query Metrics (N = 300 Queries)

k	Quad-Tree (ms)	KD-Tree (ms)	Quad-Tree QPS	KD-Tree QPS	KD vs Quad Speedup
5	0.01429	0.06667	70000	15000	0.21429
10	0.00952	0.07143	105000	14000	0.13333
20	0.00952	0.06667	105000	15000	0.14286
50	0.03810	0.06190	26250	16153.85	0.61538
100	0.09048	0.08571	11052.63	11666.67	1.05556

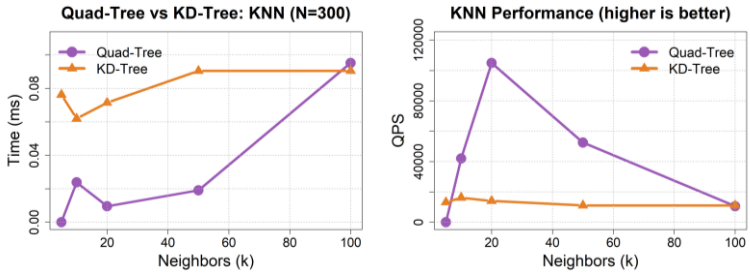

Fig. 2. Comparison between Quad-Tree and KD-Tree in KNN queries.

3.3 Statistical Evaluation

The statistical analysis reinforced the experimental performance patterns. For range queries, the Wilcoxon signed-rank test showed that Grid consistently outperformed R-Tree (W = 15, p = 0.0312), with an exceptionally large effect size (d = 203.87) and an average speedup of 181.56×, highlighting the strong advantage of uniform spatial partitioning under dense workloads. The Kruskal–Wallis test also identified significant

differences across the four indexing structures (H(3) = 16.7521, p = 0.0008), confirming their heterogeneous computational profiles. In contrast, for KNN queries, the Wilcoxon test comparing Quad-Tree and KD-Tree (W = 1, p = 0.9688) detected no significant difference, despite a large but inconsistent effect (d = –1.51). Overall performance remained balanced, with KD-Tree offering only a modest speedup (0.43×) and surpassing Quad-Tree solely at the largest neighborhood size (k = 100). Together, these results indicate that while Grid shows clear statistical superiority for range-query workloads, KNN performance is more evenly distributed across indexing methods.

3.4 Regional Performance Analysis

The regional analysis reveals pronounced spatial and productive disparities. The Selva registers the highest production (1.93 M ton) and average yield (14,534 kg/ha), with 65.1% of its area classified as high-productivity. Although the Sierra holds the largest number of crop records (53,542), its production (510,339 ton) and yield (12,038 kg/ha) are comparatively lower. The Costa presents intermediate production but the highest proportion of high-productivity zones (68.5%). In terms of spatial indexing performance, R-Tree consistently shows elevated query latency (650–750 ms), whereas the Grid index achieves near-zero execution times in the Sierra and Costa and only 10 ms in the Selva, demonstrating superior stability and scalability under dense agricultural datasets. These regional patterns, summarized in Table 5 and illustrated in Fig. 3, underscore the computational efficiency of grid-based indexing for large-scale agro-spatial analysis [12, 17].

Table 5. Regional Performance Analysis

Region	Crops	Prod (ton)	Yield (kg/ha)	HighProd (%)	R-Tree (ms)	Grid (ms)
Selva	17,039	1,932,406.68	14,534.06	65.13	750	10
Sierra	53,542	510,339.22	12,038.68	52.39	660	≈0
Costa	21,250	391,395.59	12,472.37	68.52	650	≈0

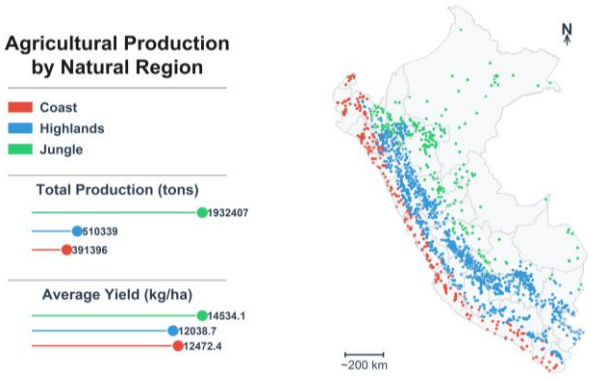

Fig. 3. Regional yield analysis.

3.5 Environmental Impact Analysis

Environmental affectations displayed clear spatial heterogeneity, with drought, pests, and frost emerging as the dominant stressors on agricultural performance. Nationally, pest incidence accounted for the largest share of impacted crop units (23.35%), followed by frost (9.08%) and drought (7.9%), underscoring the relevance of biotic and climatic pressures. To describe the spatial structure of these stressors, Table 6 outlines the Top 5 departments per affectation type based on the proportion of impacted crop units. These results support the subsequent spatial density examination (Fig. 4) and the integrated performance assessment.

Table 6. Drought Impacts (Top 6 Departments)

Aff. Type	Department	Total Crops (n)	Affected Crops (n)	Affectation (%)	Avg. Loss (%)
Drought	Cajamarca	10,398	2,260	21.73	16.85
	Lambayeque	773	101	13.07	81.99
	Áncash	6,569	699	10.64	24.14
	Tumbes	1,194	121	10.13	0.67
	Huancavelica	3,372	335	9.93	1.43
Pests	Apurímac	3,779	1,644	43.50	99.08
	Tacna	2,625	1,106	42.13	38.82
	Tumbes	1,194	436	36.52	4.22
	Huánuco	6,158	1,942	31.54	82.37
	Ayacucho	6,212	1,952	31.42	11.29
Frost	Cusco	6,344	1,750	27.59	114.06
	Puno	6,128	1,437	23.45	12.92
	Huancavelica	3,372	626	18.56	1.20
	Ayacucho	6,212	1,042	16.77	2.05
	Junín	1,496	197	13.17	164.77

Drought impacts followed an inter-Andean pattern, with Cajamarca showing the highest incidence (21.73%), followed by Lambayeque (13.07%) and Áncash (10.64%). Lambayeque recorded the most severe average losses (81.99%), highlighting critical drought stress in coastal systems, while Tumbes (10.13%) and Huancavelica (9.93%) reflected additional localized exposure.

Pest affectations were the most extensive nationally. Apurímac (43.50%) and Tacna (42.13%) presented the highest incidences, with Tumbes (36.52%), Huánuco (31.54%), and Ayacucho (31.42%) also heavily affected; Huánuco recorded high-severity losses (82.37%). These results confirm pests as the dominant stressor in magnitude and spatial concentration.

Frost impacts clustered in high-elevation zones, led by Cusco (27.59%) and Puno (23.45%), with severe losses in Cusco (114.06%). Huancavelica (18.56%) and Ayacucho (16.77%) maintained notable vulnerability, while Junín exhibited the most extreme loss estimate (164.77%), indicating near-total yield failure.

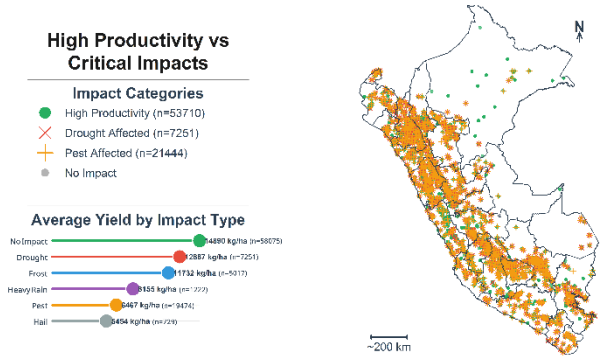

Fig. 4. Spatial distribution of drought, pest, and frost affectations across agricultural plots

3.6 Spatial Indexing Applied: Irrigation Systems, Grid, and KD-Tree

Irrigation systems exhibit marked asymmetry across the country: gravity irrigation dominates in 23 of 25 departments, while sprinkler and drip systems appear in only one department each. The largest irrigated clusters—Arequipa (5,752 units), Lima (5,139), Áncash (3,961), Moquegua (3,586), and Ica (3,055)—align consistently with the standardized 1,186-cell grid. Applying a KD-Tree algorithm (k = 100) within this grid revealed a highly compact cluster in Amazonas, where drought-affected crops spatially coincide with their nearest neighbors and major pest hotspots, indicating localized convergence of multiple stressors. Overall, the predominance of gravity irrigation combined with grid partitioning and KD-Tree clustering establishes a robust spatial framework for multi-factor agricultural risk assessment (Fig. 5).

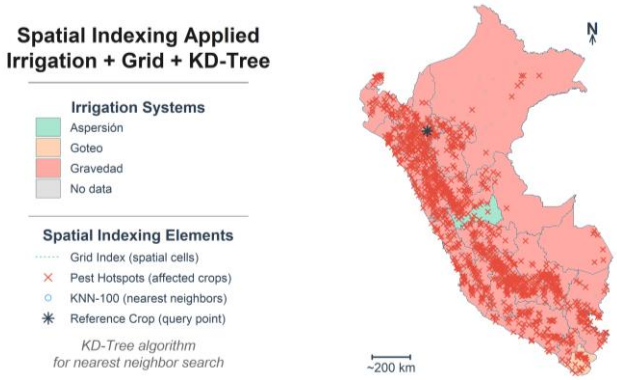

Fig. 5. Spatial indexing applied to irrigation and pests (combined hotspot visualization).

3.7 Spatial Density and Productive Patterns

The spatial density analysis identified a concentrated agricultural corridor dominated by five high-intensity zones with densities ranging from 0.1052–0.1335 crops/km². Zones 2-4 and 2-3 form the strongest cluster (>26,800 crops), while 3-2, 5-1, and 4-2

extend this axis north–south. Grid queries remained near-instant (0 ms) and R-Tree searches stable (~560–1,030 ms). These patterns outline a continuous central belt of intensified cultivation, as shown in Fig. 6, highlighting structurally cohesive production hotspots [17, 18].

Table 7. Top 5 High-Density Zones

Zone	Crops	Production (t)	Area (km²)	Density	Grid (ms)	R-Tree (ms)
2-4	13,631	737,491	102,066.94	0.1335	0	610
2-3	13,245	125,914	101,214.86	0.1309	0	1,030
3-2	13,000	50,166	100,007.44	0.1300	0	560
5-1	11,929	70,835	98,448.96	0.1212	0	640
4-2	10,519	23,204	100,007.44	0.1052	0	660

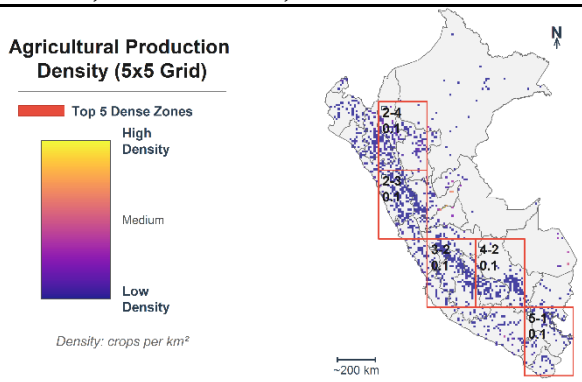

Fig. 6. Spatial agricultural density map.

4 Discussion

The results clearly establish the superiority of the Grid index over the classic R-Tree for range queries (0.1–2 km radius) on a nationwide dataset of 91 831 georeferenced agricultural plots (ENA 2024 – Peru). Grid achieved stable latencies of 3.66–3.70 ms, sustained >270 QPS, and delivered 180–183× speedups compared to R-Tree (Wilcoxon $W = 15$, $p = 0.0312$, Cohen's $d = 203.87$), while requiring virtually zero memory overhead (0.0013 MB vs 64.8 MB for R-Tree) [5, 19]. For k-nearest neighbor queries ($k = 5$–100), Quad-Tree dominated at low-to-medium k values (up to 105 000 QPS), whereas KD-Tree only marginally outperformed it at $k = 100$, with no statistically significant differences overall (Wilcoxon $p = 0.9688$) [10, 11]. These patterns confirm that simple uniform partitioning dramatically outperforms hierarchical bounding-box structures in dense, moderately homogeneous point clouds typical of national-scale agricultural registries.

A key practical contribution of this work is the seamless integration of these lightweight indexes into real-world IoT and edge-cloud environments for precision agriculture. The near-zero memory footprint and sub-4 ms range-query latency of Grid enable direct deployment on low-cost IoT gateways, LoRaWAN/ NB-IoT nodes, and mobile

devices used by agricultural extension agents, supporting real-time decision making (variable-rate irrigation, targeted pest alerts, and traceability) without requiring high-performance servers [2, 14, 20]. The combination of Grid (range) + Quad-Tree/KD-Tree (KNN) comfortably handles hundreds of concurrent queries per second from streaming sensor networks, overcoming the performance bottlenecks of traditional R-Tree variants in dynamic spatio-temporal flows [1, 2, 13]. This makes the proposed solution immediately applicable to national early-warning systems and on-farm IoT platforms in resource-constrained settings.

Regional analysis revealed marked eco-productive contrasts: the Amazon rainforest (Selva) exhibited the highest yield (14 534 kg/ha) and production (1.93 M tons) but also the highest national pest incidence (23.35 %), whereas the Andes (Sierra) concentrated the largest number of records (53 542) together with severe drought and frost exposure (Cusco 27.59 %, Puno 23.45 %). Grid maintained near-instantaneous response (≤10 ms even in the spatially dispersed Selva vs 650–750 ms for R-Tree) demonstrates remarkable robustness across two orders of magnitude in point density, a critical feature for Andean and Amazonian countries with extreme altitudinal and climatic gradients [12, 17, 21].

In conclusion, the selective Grid + Quad-Tree/KD-Tree strategy offers the best performance–memory–energy trade-off for massive agricultural spatial data management in IoT-enabled precision agriculture systems, significantly outperforming modern persistent-memory, streaming, or graph-oriented R-Tree variants [1–3, 13]. Remaining limitations (false positives due to cell discretization and bounding-box overestimation) can be addressed in future work through precise polygon indexing or hybrid learned indexes [18]. The present findings provide a solid technical foundation for the immediate modernization of national platforms such as Peru's INEI/MIDAGRI and for the scalable deployment of climate-resilient IoT precision agriculture solutions across tropical and mountainous developing regions [6, 15, 16, 20, 22].

5 Conclusions

Tree/KD-Tree, dramatically outperforms the classic R-Tree on a nationwide Peruvian agricultural dataset (91 831 georeferenced ENA 2024 records), achieving 180–183× speedups and >270 QPS in range queries (3.66–3.70 ms), near-zero memory usage (0.0013 MB), and full stability across highly heterogeneous regions (≤10 ms even in the dispersed Amazon rainforest). Statistical tests (Wilcoxon $p = 0.0312$, $d = 203.87$; Kruskal-Wallis $p = 0.0008$) confirm the overwhelming superiority of uniform partitioning for dense real-world agricultural workloads.

The proposed solution is immediately deployable on low-cost IoT and edge-cloud infrastructures, enabling real-time national-scale precision agriculture applications: early warning of drought/pest/frost convergence, variable-rate management zones, and climate-resilient decision making. These advances provide a practical, scalable blueprint for modernizing public systems such as Peru's INEI/MIDAGRI registries and for extending IoT-enabled, data-driven agricultural intelligence across tropical and Andean developing countries [1, 13, 18, 19].

References

1. Kim J, Hong S, Jeong S, et al (2024) SGIR-Tree: Integrating R-Tree Spatial Indexing as Subgraphs in Graph Database Management Systems. ISPRS International Journal of Geo-Information 2024, Vol 13, 13:. https://doi.org/10.3390/IJGI13100346
2. Peng W, Chen L, Ouyang X, Xiong W (2024) A Time-Identified R-Tree: A Workload-Controllable Dynamic Spatio-Temporal Index Scheme for Streaming Processing. ISPRS International Journal of Geo-Information 2024, Vol 13, 13:. https://doi.org/10.3390/IJGI13020049
3. Xia J, Huang S, Zhang S, et al (2020) DAPR-tree: a distributed spatial data indexing scheme with data access patterns to support Digital Earth initiatives. Int J Digit Earth 13:1656–1671. https://doi.org/10.1080/17538947.2020.1778804;WGROUP:STRING:PUBLICATION
4. Zhu Q, Gong J, Zhang Y (2007) An efficient 3D R-tree spatial index method for virtual geographic environments. ISPRS Journal of Photogrammetry and Remote Sensing 62:217–224. https://doi.org/10.1016/J.ISPRSJPRS.2007.05.007
5. Mao Q, Qader MA, Hristidis V (2023) Comparison of LSM indexing techniques for storing spatial data. Journal of Big Data 2023 10:1 10:51-. https://doi.org/10.1186/S40537-023-00734-3
6. Sandonís-Pozo L, Llorens J, Escolà A, et al (2022) Satellite multispectral indices to estimate canopy parameters and within-field management zones in superintensive almond orchards. Precision Agriculture 2022 23:6 23:2040–2062. https://doi.org/10.1007/S11119-022-09956-6
7. Colaço AF, Molin JP, Rosell-Polo JR, Escolà A (2018) Spatial variability in commercial orange groves. Part 1: canopy volume and height. Precision Agriculture 2018 20:4 20:788–804. https://doi.org/10.1007/S11119-018-9612-3
8. Colaço AF, Molin JP, Rosell-Polo JR, Escolà A (2018) Spatial variability in commercial orange groves. Part 2: relating canopy geometry to soil attributes and historical yield. Precision Agriculture 2018 20:4 20:805–822. https://doi.org/10.1007/S11119-018-9615-0
9. Huang PW, Lin PL, Lin HY (2001) Optimizing storage utilization in R-tree dynamic index structure for spatial databases. Journal of Systems and Software 55:291–299. https://doi.org/10.1016/S0164-1212(00)00078-9
10. Samet H (1990) The design and analysis of spatial data structures. The design and analysis of spatial data structures. https://doi.org/10.1016/0924-2716(91)90007-i
11. Bentley JL (1975) Multidimensional binary search trees used for associative searching. Commun ACM 18:509–517. https://doi.org/10.1145/361002.361007
12. Serrao L, Giovannini L, Terrones LEB, et al (2025) Integrating farmers' perceptions into climate change assessment in the data-scarce Peruvian Amazon.

Climatic Change 2025 178:3 178:55-. https://doi.org/10.1007/S10584-025-03891-X

13. Lavinsky B, Zhang X (2022) PM-Rtree: A Highly-Efficient Crash-Consistent R-tree for Persistent Memory. ACM International Conference Proceeding Series. https://doi.org/10.1145/3538712.3538713;WGROUP:STRING:ACM
14. Zhou Y, De S, Wang W, et al (2017) Spatial Indexing for Data Searching in Mobile Sensing Environments. Sensors 2017, Vol 17, 17:. https://doi.org/10.3390/S17061427
15. Omia E, Bae H, Park E, et al (2023) Remote Sensing in Field Crop Monitoring: A Comprehensive Review of Sensor Systems, Data Analyses and Recent Advances. Remote Sensing 2023, Vol 15, 15:. https://doi.org/10.3390/RS15020354
16. Xu J, Cui Y, Zhang S, Zhang M (2024) The evolution of precision agriculture and food safety: a bibliometric study. Front Sustain Food Syst 8:1475602. https://doi.org/10.3389/FSUFS.2024.1475602/FULL
17. Móstiga M, Armenteras D, Vayreda J, Retana J (2024) Decoding the drivers and effects of deforestation in Peru: a national and regional analysis. Environment, Development and Sustainability 2024 27:7 27:17395–17415. https://doi.org/10.1007/S10668-024-04638-X
18. Wang C, Yu J, Zhao Z (2022) GLIN: A (G)eneric (L)earned (In)dexing Mechanism for Complex Geometries. Woodstock '18: ACM Symposium on Neural Gaze Detection, June 03â•fi05, 2018, Woodstock, NY 1:. https://doi.org/10.1145/1122445.1122456
19. Guttman A (1984) R-trees: A dynamic index structure for spatial searching. Proceedings of the ACM SIGMOD International Conference on Management of Data 47–57. https://doi.org/10.1145/602259.602266;CSUBTYPE:STRING:CONFERENCE
20. San Emeterio de la Parte M, Martínez-Ortega JF, Hernández Díaz V, Martínez NL (2023) Big Data and precision agriculture: a novel spatio-temporal semantic IoT data management framework for improved interoperability. Journal of Big Data 2023 10:1 10:52-. https://doi.org/10.1186/S40537-023-00729-0
21. Mader C, Godde P, Hägele E, et al (2025) Mapping and Geospatial Analysis of Ancient Terrace Agricultural Systems in Lucanas Province, Peruvian Andes, Based on Satellite Imagery, High-Resolution DSMs, and Field Surveys. Geoarchaeology 40:e70002. https://doi.org/10.1002/GEA.70002;PAGE:STRING:ARTICLE/CHAPTER
22. Espinel R, Herrera-Franco G, García JLR, Escandón-Panchana P (2024) Artificial Intelligence in Agricultural Mapping: A Review. Agriculture 2024, Vol 14, 14:. https://doi.org/10.3390/AGRICULTURE14071071